SI Appendix

Different phospho-isoforms of RNA polymerase II engage the Rtt103 termination factor in a structurally analogous manner

Corey M. Nemec, Fan Yang, Joshua M. Gilmore, Corinna Hintermair, Yi-Hsuan Ho, Sandra C. Tseng, Martin Heidemann, Ying Zhang, Laurence Florens, Audrey P. Gasch, Dirk Eick, Michael P. Washburn, Gabriele Varani, and Aseem Z. Ansari*

Correspondence should be addressed to Aseem Z. Ansari (azansari@wisc.edu)

Supplementary Materials and Methods

Northern blot. 25mL cultures were grown to OD 0.5, pelleted, resuspended in TE lysis buffer (10mM Tris-HCl pH 7.5, 10mM EDTA, 0.5% SDS) and flash frozen. The following day, cells were thawed, and RNA was extracted with 700 µL hot phenol. 2 µL GlycoBlue was added to the aqueous layer, and RNA was extracted again. 700 µL chloroform was added to the aqueous layer and was added to a Heavy Phase Lock Gel Tube and spun for 5 minutes at room temp (16,000 g). RNA was precipitated from the aqueous layer with 10% 3M NaOAc and 2.5 volumes cold 100% EtOH and frozen at -80 °C overnight. The next day, RNA was pelleted, washed with 70% EtOH and resuspended in 50 µL RNase-free water. 20 µg RNA was run on a 1.5% agarose gel in 1X MOPS, 6% formaldehyde. RNA was transferred to Hybond-N membrane overnight using 20x SSC buffer and was crosslinked to the membrane via UV irradiation. Primers were designed to *SNR33* (1), *SNR40*, and *SCR1*, containing a T7 promoter for in vitro transcription of a radioactive probe (Table S3). ^{32}P-UTP was incorporated into probes via in vitro transcription (AmpliScribe T7-Flash transcription kit – Epicentre). G25 columns (GE Healthcare) were used to remove unincorporated UTP. Blots were incubated in ULTRAhyb solution (Ambion) at 68°C for 30 minutes prior to addition of the radioactive probe overnight. Blots were washed twice with 2x SSC, 0.1% SDS and twice with 0.1x SSC, 0.1% SDS. Phosphorimage screens were exposed overnight and scanned the next morning on a Typhoon FLA9000 (GE Healthcare).

Fisher's exact test

To determine if snoRNAs with readthrough defects were enriched at terminal snoRNAs, a Fisher's exact test was performed. The null hypothesis assumes that snoRNAs with readthrough defects are equally likely to be terminal snoRNAs (i.e. monocistronic or the terminal snoRNA of a polycistronic snoRNA) or internal snoRNAs (i.e. internal polycistronic snoRNA or snoRNAs in introns). A contingency table based on Fig. 2D is shown.

	Terminal snoRNA	**Internal snoRNA**	Totals
Readthrough snoRNA in T4A	**36**	**1**	37 readthrough
Non-readthrough snoRNA in T4A	**21**	**19**	40 non-readthrough
Totals	57 terminal	20 internal	77 snoRNAs

The hypergeometric p-value of 3.3×10^{-6} suggests that the null hypothesis can be rejected.

Chromatin immunoprecipitation. ChIP was done as previously described with minor modifications (2). Cells were grown in rich media to OD_{600} ~0.5, crosslinked, pelleted, and flash frozen. Cells were lysed in lysis buffer (50mM HEPES-KOH, 140mM NaCl 1mM EDTA, 1%

Triton X-100, 0.1% Na-Deoxycholate), with freshly added protease inhibitors (1 mM PMSF, 1 mM benzamidine, 1.45 mM pepstatin), and 1 mM freshly added phosphatase inhibitors (NaF, NaN_3, and Na_3VO_4). Chromatin was sonicated on a Misonix 4000 sonicator, input was reserved, chromatin was immunoprecipitated overnight with 3 µL α-Rpb3 (W0012 from Neoclone, currently BioLegend), 10 µL α-pThr4 (1G7), or 5 µL α-FLAG (Sigma). DNA was reverse crosslinked, amplified, and labeled using ligation-mediated PCR, and was hybridized to full yeast genome tiled microarrays (NimbleGen). The arrays have ~380,000 probes of 51 nucleotides offset by 32 base pairs across non-repetitive regions of the genome (2, 3). Data were normalized as previously described (2). In Figure 2, pThr4 and pSer2 are normalized to Rpb3. pSer2 traces were re-analyzed from ref. (2). ChIP experiments in Fig. S4*A* were reanalyzed from refs. (4, 5). ChIP experiments in S4B were quantile normalized to compare ChIPs from different experiments (WT vs T4A) on the same graph. ChIP experiments in Fig. S4*C* were reanalyzed from (GSE72802). Htz1 ChIP data in Fig. S4*D* was reanalyzed from ref. (6).

Co-immunoprecipitation and label-free quantitative proteomics. WT, T4A, T4E (unshuffled), and Z26 were grown in two liters of selective media. Cultures were grown to an OD_{600} ~1.0, pelleted, and filtered onto Whatman filter paper. Cells were scraped directly into liquid nitrogen, briefly shaken, and frozen at -80 °C. Flash frozen cells were loaded into a 50 mL grinding jar with a grinding ball and immersed into liquid nitrogen. Grinding jars were loaded into a Retsch Mixer Mill MM 400, and cells were pulverized for six cycles (3' at 15 Hz), and grinding jars were re-immersed in liquid nitrogen between each round. Lysed yeast powder was dissolved in 10 mL 1X NET-seq buffer (7) (20 mM HEPES, pH 7.4, 110 mM KOAc, 0.5% Triton X-100, 0.1% Tween-20, 10 mM $MnCl_2$), with freshly added protease inhibitors (1 mM PMSF, 1 mM benzamidine, 1.45 mM pepstatin), 1 mM freshly added phosphatase inhibitors (NaF, NaN_3, and Na_3VO_4), and 2,000 U DNase (Sigma), and nutated at 4 °C for 30 minutes. Debris was pelleted for 10 minutes at 4,000 RPM, and lysate was incubated with 200 µL anti-HA Dynabeads (Life Technologies). Following three washes with NET-seq buffer, samples were eluted with thrice with 100 µL HA peptide (2 mg/mL in TBS) at room temp for 30 minutes. Fractions were combined, and 100 µL 100mM Tris-HCl pH 8.5 and 100 µL cold TCA was added and nutated overnight. Protein was precipitated and washed twice with cold acetone. Triplicate samples were analyzed by label-free quantitative proteomics analysis as previously described (8). Significant proteins were identified using QSpec (9). Proteins identified in all three replicates of the negative control (Z26) were discarded from analysis.

Purification of TAP-tagged proteins. Cells expressing C-terminally TAP-tagged proteins (10) were grown to OD_{600} ~ 1.0 in 1 L selective media. Cells were pelleted and lysed in TAP buffer A (20 mM HEPES pH 7.9, 300 mM potassium acetate, 0.5 mM EDTA pH 8.0, 10% glycerol, 0.05% NP40) with freshly added protease inhibitors (1 mM PMSF, 1 mM benzamidine, 1.45 mM pepstatin), via bead beating with silica beads (OPS Diagnostics). Cell debris was pelleted, and protein complexes were immunoenriched with 200 µL of a 50/50 slurry of IgG-sepharose 6 Fast Flow beads (GE-Healthcare) in TAP buffer A. After 3 hours nutating at 4°C, beads were pelleted and washed five times with TAP buffer A and eluted overnight in 100 µL TAP buffer A with 1mM DTT and 120 U TEV protease (Sigma).

Purification of GST-CTD. The CTD substrate, GST-CTD14 (fourteen repeats of YSPTSPS fused to GST) was expressed in BL21(DE3). Cells were grown to midlog phase at 37°C and induced with 1 mM IPTG overnight at 16°C. Cells were pelleted (5,000 g for 20 minutes) and resuspended in 5 mL Buffer B (1X PBS, 10% glycerol, 0.01% NP40) with freshly added 1 mM protease inhibitors (PMSF, benzamidine, pepstatin). Cells were lysed with 3 rounds of sonication at power level 5 using a Heat Systems-Ultrasonics Inc. W-220 Sonicator. Cell debris

was pelleted at 13,000 rpm for 20 minutes at 4°C and a 200 µL 50/50 slurry of Gutathione-Sepharose 4B beads (GE-Healthcare) in Buffer B was added to the supernatant. After 3 hours nutating at 4°C, beads were pelleted and washed once with Buffer B. Beads were resuspended in 1 mL FastAP buffer (10 mM Tris-HCl pH 8.0, 5 mM $MgCl_2$, 100 mM KCl, 0.02% TritonX-100, 100 ug/mL BSA) and incubated with 100 U FastAP Thermosensitive Alkaline Phosphatase (Thermo Scientific) for 1 hour at 37°C. Beads were washed five times with Buffer B. CTD bound to beads were phosphorylated (or mock treated) and incubated with 30 µL TAP-purified Rtt103(WT) or Rtt103(R108N) with 30 µL TAP buffer A for 3 hours at 23 °C. Beads were washed three times with TAP buffer A and eluted via boiling in SDS sample buffer.

Western blot analysis of yeast CTD marks. WT, S2A/WT, and T4A cells were grown to an OD_{600} of 1.0 in 5 mL YPD. Cells were pelleted and lysed in 300 µL lysis buffer (50 mM HEPES-KOH, 140 mM NaCl, 1 mM EDTA, 1% Triton X-100, 0.1% Na-deoxycholate) with freshly added protease inhibitors (1 mM PMSF, 1 mM benzamidine, 1.45 mM pepstatin), and 1 mM freshly added phosphatase inhibitors (NaF, NaN_3, and Na_3VO_4). Extract was sonicated (Heat Systems-Ultrasonics Sonicator W-220) once for 30 seconds on power level 4. Debris was pelleted, and HA-tagged Pol II was incubated with 50 µL α-HA magnetic beads (MBL) at 4 °C for 30 minutes. Beads were washed thrice with lysis buffer, and eluted via boiling in 50 µL lysis buffer with SDS loading dye.

Western blot analysis of human CTD marks. B-cell line Raji, which conditionally expresses the HA-tagged, alpha-amanitin resistant, large subunit Rpb1 of Pol II was used to analyze the impact of CTD mutants on Pol II CTD phosphorylations. These recombinant Pol II have their CTD replaced by an artificial one composed of the WT 1-3, repeat 52, and with 48 repeats cloned between them. The repeats are either the consensus sequence (con 48), or contain alanine substitutions at each Ser2 (S2A 48) or Thr4 (T4A 48). Western blot analysis of Raji whole cell extracts 48h after induction and 24h after α-amanitin using mAbs specific for pSer2 (3E10), pThr4 (6D7), pSer5 (3E8), or Rpb1 (Pol3.3).

Supplementary Tables

Table S1 snoRNA 3' extension indices. snoRNA gene boundaries were obtained from SGD. The 3' extension index is defined as the fold change in the average expression 200 base pairs downstream of the 3' end of snoRNAs as described previously (11). Extension indices for T4A, S2A/WT, and *paf1Δ* are listed. Pol II readthrough is defined as the fold change in Pol II occupancy in the 1kb window downstream of the 3' end of snoRNAs between the pcf11-13 mutant and the WT control at the non-permissive 37°C. Data was reanalyzed from (12).

	RNA 3' extension index			Pol II readthrough
	T4A	S2A/WT	*paf1Δ*	pcf11-13
SNR47	20.56317	1.206106	2.327812	0.666014
SNR33	20.55386	1.651381	2.1752	0.709008
SNR13	18.57099	0.949022	1.117714	0.650981
SNR5	16.24483	1.197944	1.900187	0.893293
SNR71	14.75729	1.306495	6.28089	0.369057
SNR81	10.42335	1.288129	3.753336	0.892775
SNR82	10.10541	1.099091	1.725318	0.47798
SNR161	7.958769	1.351605	4.7699	1.005122
SNR64	7.321756	1.4818	3.05996	0.758007
SNR48	7.257963	1.404193	8.603942	0.622283
SNR51	6.985045	0.86254	2.368415	0.554743
SNR60	6.018166	1.457367	3.856852	0.525908
SNR189	5.29075	1.197957	1.564967	0.653558
SNR49	4.924767	1.609617	0.960357	0.367708
SNR42	4.832681	1.59369	2.292911	0.720548
SNR68	4.551981	1.293856	2.354765	0.613346
SNR69	4.255688	1.312453	1.856208	0.499878
SNR43	3.757345	1.386398	0.646973	0.570838
SNR50	3.671672	0.980826	1.603734	0.584816
SNR63	3.415066	1.071335	0.699095	0.475786
SNR85	3.351023	0.978456	3.520542	0.637893
SNR79	3.040767	0.954554	2.826278	0.491831
SNR53	2.657638	1.174924	2.304851	0.462591
SNR56	2.313384	1.208007	2.128699	0.462851
SNR34	2.235882	1.121615	1.720714	0.662099
SNR4	2.210041	0.907664	0.981142	0.777451
SNR58	2.148059	1.005541	1.555845	1.165614
SNR66	2.059697	0.668658	0.659118	0.488941
SNR9	2.036505	1.543804	1.627175	0.843035
SNR46	2.033816	1.130491	0.862743	0.621357
SNR30	1.970041	1.303056	1.548273	0.667513
SNR59	1.906974	0.784911	1.026546	0.502385
SNR8	1.894283	1.196421	1.16092	0.631439
SNR87	1.880333	0.870813	0.24625	1.159246

SNR72	1.780121	0.498967	0.826861	0.505331
SNR3	1.747688	1.224257	1.467941	0.497953
SNR11	1.706873	1.28778	0.951301	0.408135
SNR39B	1.624917	1.223926	1.474269	0.53027
SNR32	1.443113	1.250063	2.890574	0.502713
SNR35	1.30877	1.421338	1.283524	0.476685
SNR83	1.262448	1.034048	1.251385	0.527469
SNR44	1.242716	0.796058	0.549081	0.357111
SNR45	1.176883	1.056141	4.312417	0.674944
SNR65	1.077019	1.062419	0.823463	0.601139
SNR70	1.061637	0.538118	1.166555	0.454555
SNR61	1.049645	0.450299	0.395043	0.528444
SNR84	1.040312	0.851025	1.631498	0.64989
SNR38	0.976409	1.046269	1.538315	0.361409
SNR36	0.972757	1.147275	0.803858	0.551321
SNR24	0.967965	0.993225	0.656882	0.38962
SNR128	0.962825	1.007215	0.883489	0.544293
SNR74	0.950202	1.207259	0.726781	0.383913
SNR75	0.943053	1.150957	0.585104	0.392611
SNR41	0.929409	1.1601	1.255554	0.416316
SNR191	0.921735	0.864665	2.794355	0.373874
SNR10	0.921432	1.079127	0.754896	0.573796
SNR73	0.917162	1.139654	0.637368	0.409634
SNR78	0.909605	0.950999	1.289798	0.467398
SNR18	0.901538	0.914687	1.155698	0.474036
SNR39	0.888747	0.766368	1.222638	0.457928
SNR76	0.880537	1.094318	0.856487	0.370382
SNR190	0.873966	1.362339	1.162437	0.492862
SNR37	0.84623	1.12023	0.561902	0.584928
SNR31	0.84618	1.074139	0.459989	0.719446
SNR52	0.837812	1.025111	1.133171	1.035289
SNR17B	0.820676	1.116889	0.409024	0.170537
SNR17A	0.792554	1.074234	1.63761	0.391032
SNR40	0.782292	1.091329	1.467107	0.325176
SNR54	0.774647	0.853166	2.121082	0.402428
SNR55	0.704681	0.827647	0.989353	0.470277
SNR86	0.701688	0.83756	1.787192	0.505481
SNR62	0.701144	1.25994	1.038977	0.685915
NME1	0.645884	0.679447	1.090526	0.428095
SNR77	0.64178	0.936685	0.868101	0.397888
SNR67	0.637734	0.885249	0.314283	0.395311
SNR80	0.56347	0.759473	0.435406	0.478915
SNR57	0.554598	0.783837	0.906104	0.469738

Table S2 Strains used in this study

Strain	Genotype	Plasmid	Reference
Z26	MATα his3Δ200 leu2-3,112 ura3-52 rpb1Δ187::HIS3	pRP112 (Rpb1 URA3)	(13)
consWT	MATα his3Δ200 leu2-3,112 ura3-52 rpb1Δ187::HIS3	pY1 (Rpb1 CTD WT21 LEU2)	This study
T4A	MATα his3Δ200 leu2-3,112 ura3-52 rpb1Δ187::HIS3	pY1 (Rpb1 CTD T4A19 LEU2)	This study
T4E	MATα his3Δ200 leu2-3,112 ura3-52 rpb1Δ187::HIS3	pY1 (Rpb1 CTD T4E23 LEU2)	This study
WT/T4A	MATα his3Δ200 leu2-3,112 ura3-52 rpb1Δ187::HIS3	pY1 (Rpb1 CTD WT11-T4A11 LEU2)	This study
T4A/WT	MATα his3Δ200 leu2-3,112 ura3-52 rpb1Δ187::HIS3	pY1 (Rpb1 CTD T4A4-WT10 LEU2)	This study
S2A/WT	MATα his3Δ200 leu2-3,112 ura3-52 rpb1Δ187::HIS3	pY1 (Rpb1 CTD S2A8-WT7 LEU2)	(14)
consWT-Rtt103-FLAG	MATα his3Δ200 leu2-3,112 ura3-52 rpb1Δ187::HIS3 rtt103::rtt103-rtt103-5xFLAG KanMX	pY1 (Rpb1 CTD WT21 LEU2)	This study
T4A-Rtt103-FLAG	MATα his3Δ200 leu2-3,112 ura3-52 rpb1Δ187::HIS3 rtt103::rtt103-rtt103-5xFLAG KanMX	pY1 (Rpb1 CTD T4A19 LEU2)	This study
Rtt103-TAP	MATa, ura3Δ0, leu2Δ0, his3Δ1, met15Δ0, rtt103-TAP::HIS3		GE-Healthcare
Rtt103(R108N)-TAP	MATa, ura3Δ0, leu2Δ0, his3Δ1, met15Δ0, rtt103(R108N)-TAP::HIS3		(15)
Paf1-TAP	MATa, ura3Δ0, leu2Δ0, his3Δ1, met15Δ0, paf1-TAP::HIS3		GE-Healthcare
Tpk1-TAP	MATa, ura3Δ0, leu2Δ0, his3Δ1, met15Δ0, tpk1-TAP::HIS3		GE-Healthcare
Set2-TAP	MATa, ura3Δ0, leu2Δ0, his3Δ1, met15Δ0, set2-TAP::HIS3		GE-Healthcare

Table S3 Oligonucleotides used in this study

Name	Function	Sequence (5'-3')
consWT-F	CTD construct	P-CCGAGCTATAGTCCAACTTCA
consWT-R	CTD construct	P-TCGGTGAAGTTGGACTATAGC
T4A-F	CTD construct	P-CCGAGCTATAGTCCAGCTTCA
T4A-R	CTD construct	P-TCGGTGAAGCTGGACTATAGC
T4E-F	CTD construct	P-CCGAGCTATAGTCCAGAATCA
T4E-R	CTD construct	P-TCGGTGATTCTGGACTATAGC
SNR33-F	Northern Probe	CGGAACGGTACATAAGAATAGAAGAG
SNR33-R	Northern Probe	TAATACGACTCACTATAGGTAAAGAAAACGATAAGAACTAACC
SNR40-F	Northern Probe	AGTACCTTAACACATGACGAAGA
SNR40-R	Northern Probe	TAATACGACTCACTATAGGCTGATCTATTTCACGCCCAGA
SCR1-F	Northern Probe	AGGCTGTAATGGCTTTCTGGTGGGA
SCR1-R	Northern Probe	TAATACGACTCACTATAGGATATGTGCTATCCCGGCCGCCTCCA

Supplementary Figures

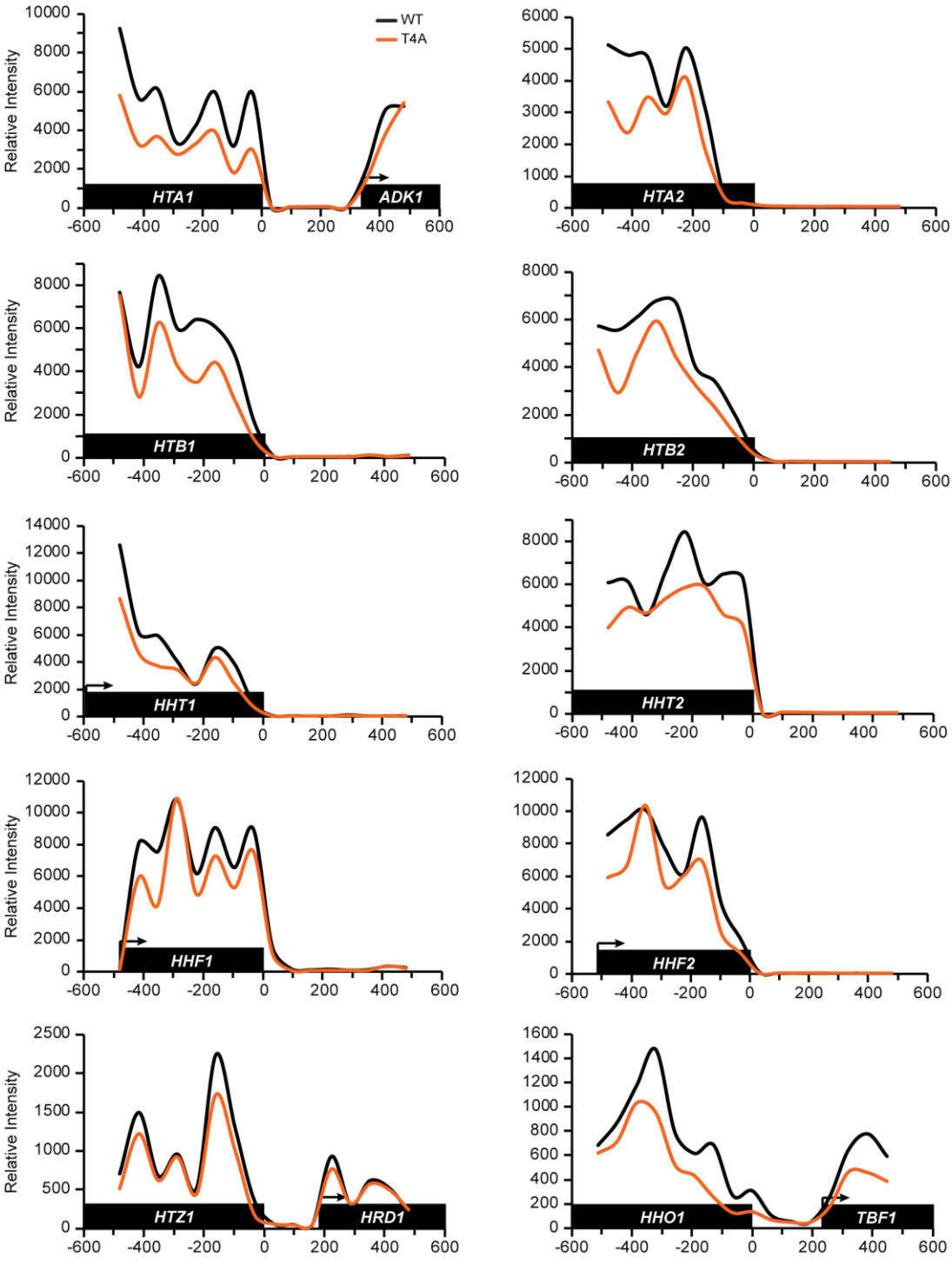

Fig. S1 T4A does not display defects at histone genes. RNA expression analysis of WT or T4A using high density genome tiling microarrays, centered at the 3'-end of histone genes. Black boxes refer to gene bodies. Arrows refer to transcription start sites. No evidence of readthrough is observed at any histone gene.

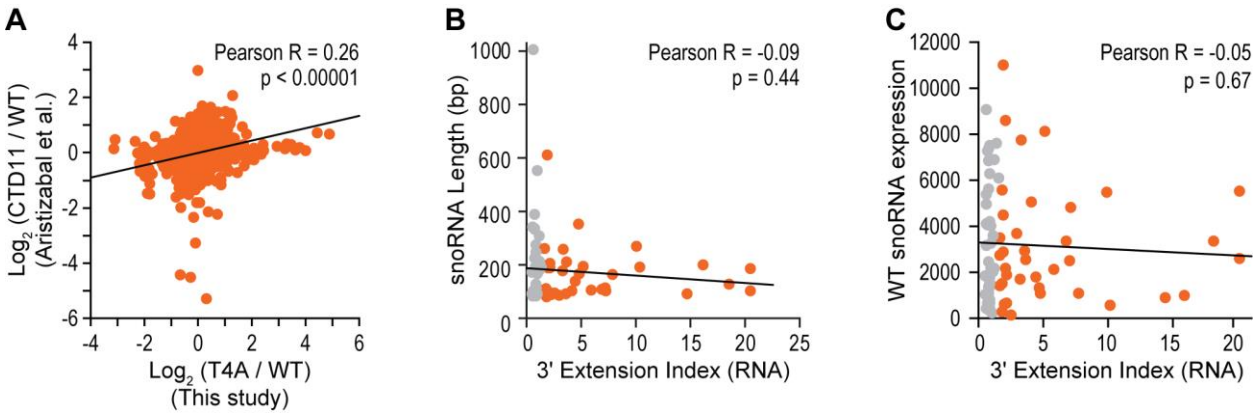

Fig. S2 Low correlation between T4A and short CTD, or between snoRNA readthrough and snoRNA length/expression. (*A*) Correlation between T4A and short CTD. The average expression fold change (T4A/WT) from high density genome tiling arrays was calculated and compared to expression data from cells bearing an 11-repeat CTD (16). (*B*) Correlation between snoRNA length and 3' extension index in T4A. (*C*) Correlation between WT snoRNA expression levels and 3' extension index in T4A.

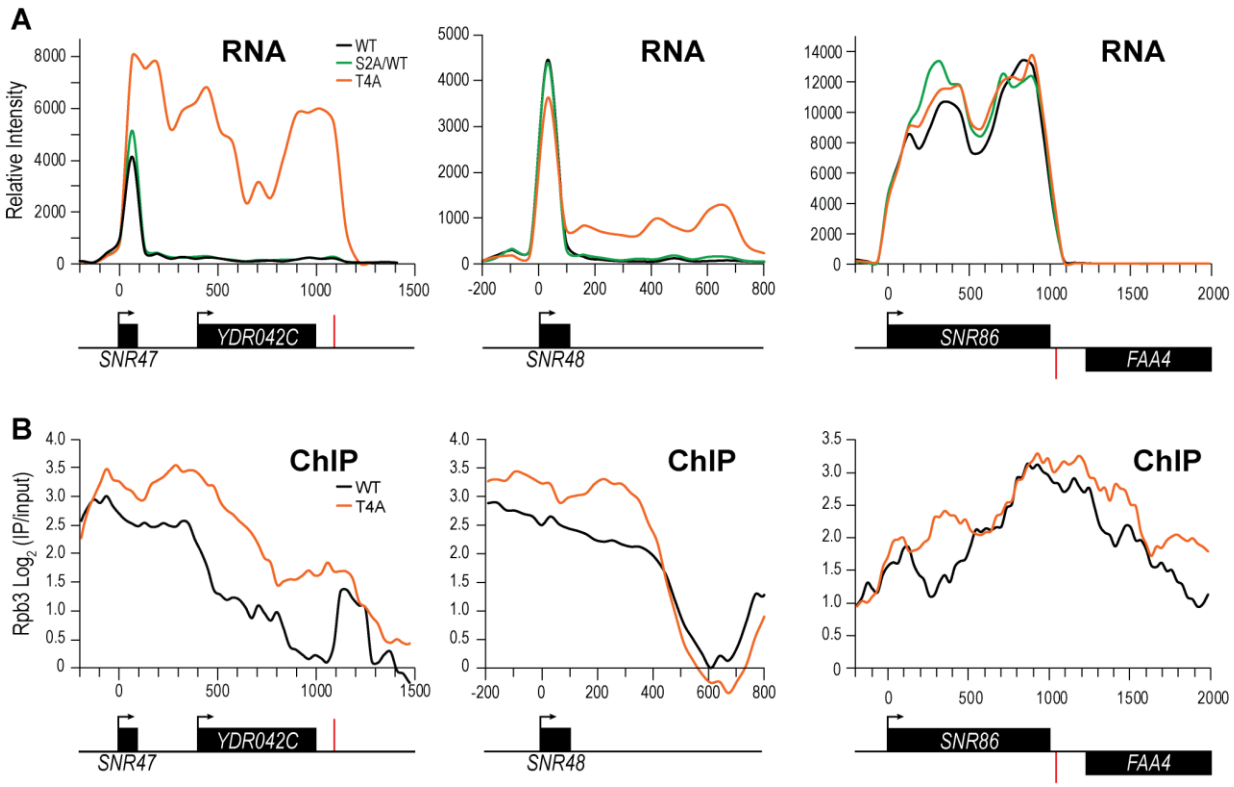

Fig. S3 Additional evidence of readthrough in T4A. (*A*) Examples of RNA traces or (*B*) Rpb3 ChIP traces at *SNR47*, *SNR48*, and *SNR86*. Readthrough was observed for *SNR47* and *SNR48* by both RNA expression analysis ChIP using high density genome tiling microarrays. No evidence of significant readthrough was observed for *SNR86* using either method. Arrows denote transcription start sites, black boxes indicate gene bodies, and red bars indicate termination sites of protein-coding genes.

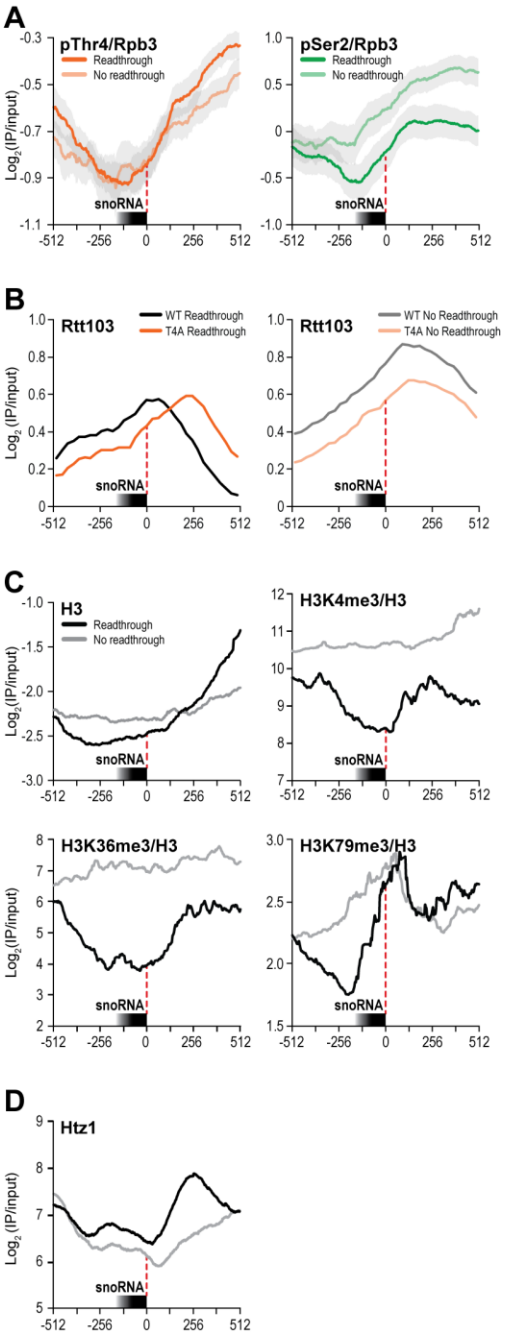

Fig. S4 Additional ChIP traces. (*A*) Metagene analysis of ChIP occupancy of pThr4 (orange) or pSer2 (green) normalized to Rpb3 centered at the 3'-end of snoRNAs either read through in T4A (dark) or not read through (light) (analyzed from refs. (4, 5)). 95% confidence intervals are shown in grey. (*B*) Metagene analysis of ChIP occupancy of Rtt103 centered at the 3'-end of snoRNAs. ChIPs were performed in WT (black) or T4A (orange), and traces are an average of ChIP occupancy across snoRNAs either read through in T4A (dark) or not read through (light). (*C*) Metagene analysis of the ChIP occupancy of histone H3 or its modifications (GSE72802) centered at the 3'-end of snoRNAs either read through in T4A (black) or not read through (grey). (*D*) Metagene analysis of the ChIP occupancy of Htz1 (6) centered at the 3'-end of snoRNAs either read through in T4A (black) or not read through (grey).

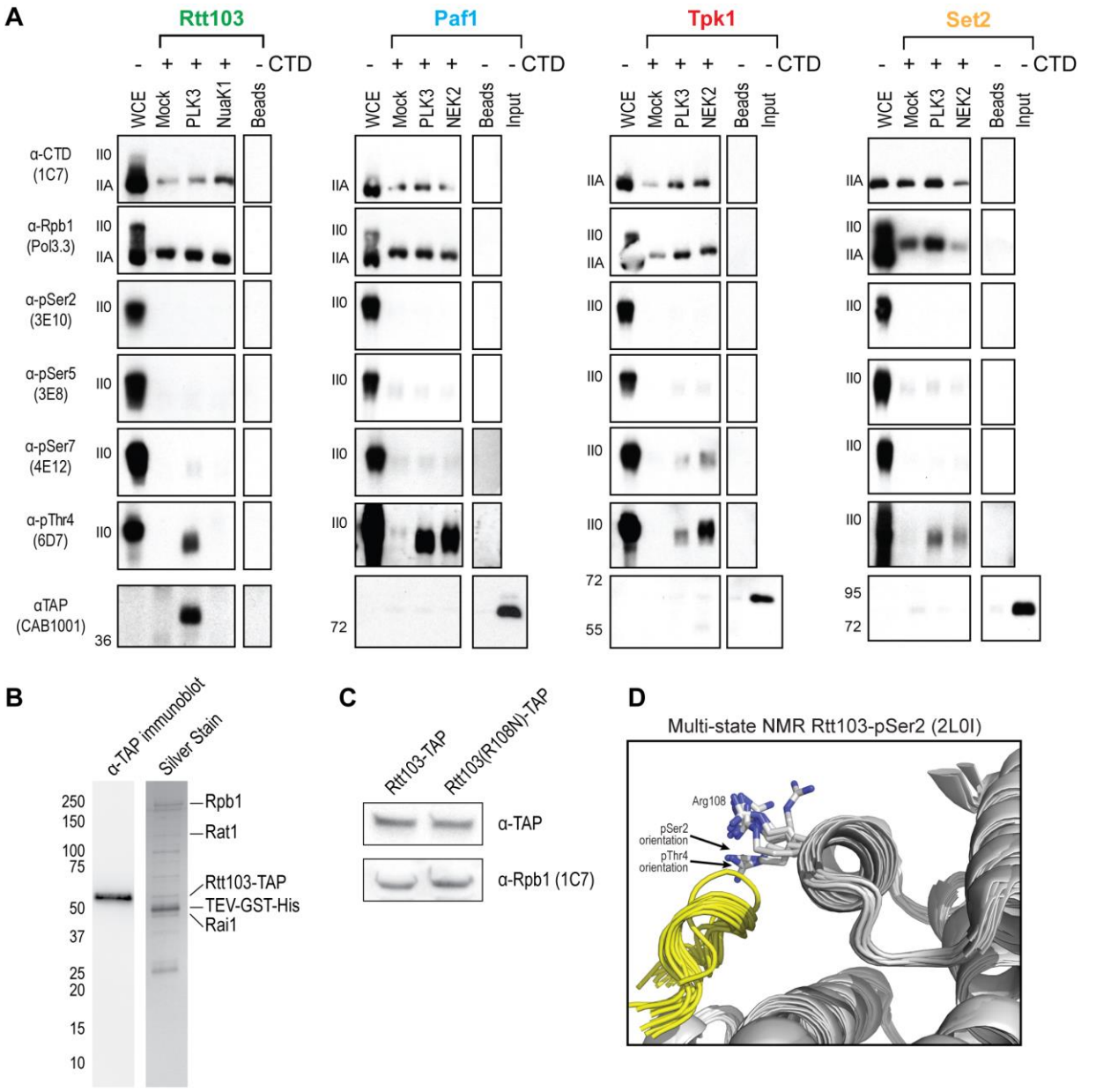

Fig. S5 Expanded evidence of binding. (*A*) Pol II bearing unphosphorylated CTD was immunoprecipitated from HeLa cell extract using 1C7 antibody and was treated with either human PLK3, NuaK1, or NEK2 to place differential phosphorylation patterns on the CTD (mock is untreated). TAP-tagged proteins were purified and incubated with the substrate. Eluted proteins were resolved via SDS-PAGE and probed with antibodies targeting Pol II, the CTD, or the TAP-tag as indicated. (*B*) TAP-tagged proteins were purified as described in the SI Materials and Methods. Immunoblot targeting the TAP-tag (CAB1001) and a silver stain are shown to illustrate purity. Identities of co-immunoprecipitated proteins were inferred from the mass of known interactors. (*C*) Immunoblots of extract from Rtt103-TAP or the Rtt103(R108N)-TAP mutant strained were probed with α-TAP (CAB1001) or α-Rpb1 (1C7) as a loading control. WT and mutant forms of Rtt103 were observed at equal abundances. (*D*) Conformation of the Arg108 side chain in the complex of Rtt103 with pSer2-CTD (15). Arg108 rotamers in (Fig. 5*A* and *B*) are labeled.

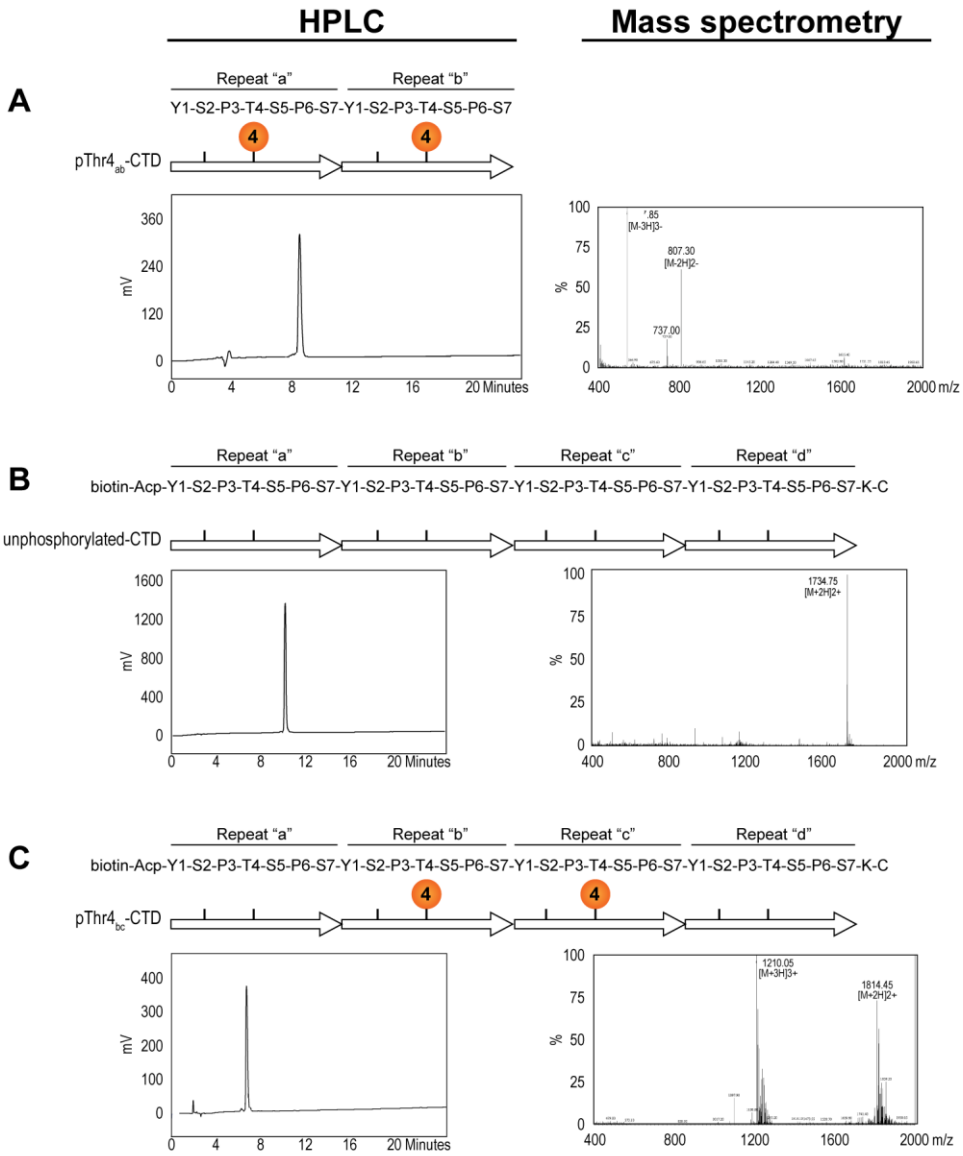

Fig. S6 Validation of CTD peptides. HPLC (left) and mass spectrometry (right) confirming synthesis of (*A*) pThr4$_{ab}$-CTD (from Fig 4*A*), (*B*) four repeat unphosphorylated CTD, and (*C*) four repeat pThr4$_{bc}$-CTD. Sequences of the peptides are shown on the top. Phosphothreonines are indicated by orange circles.

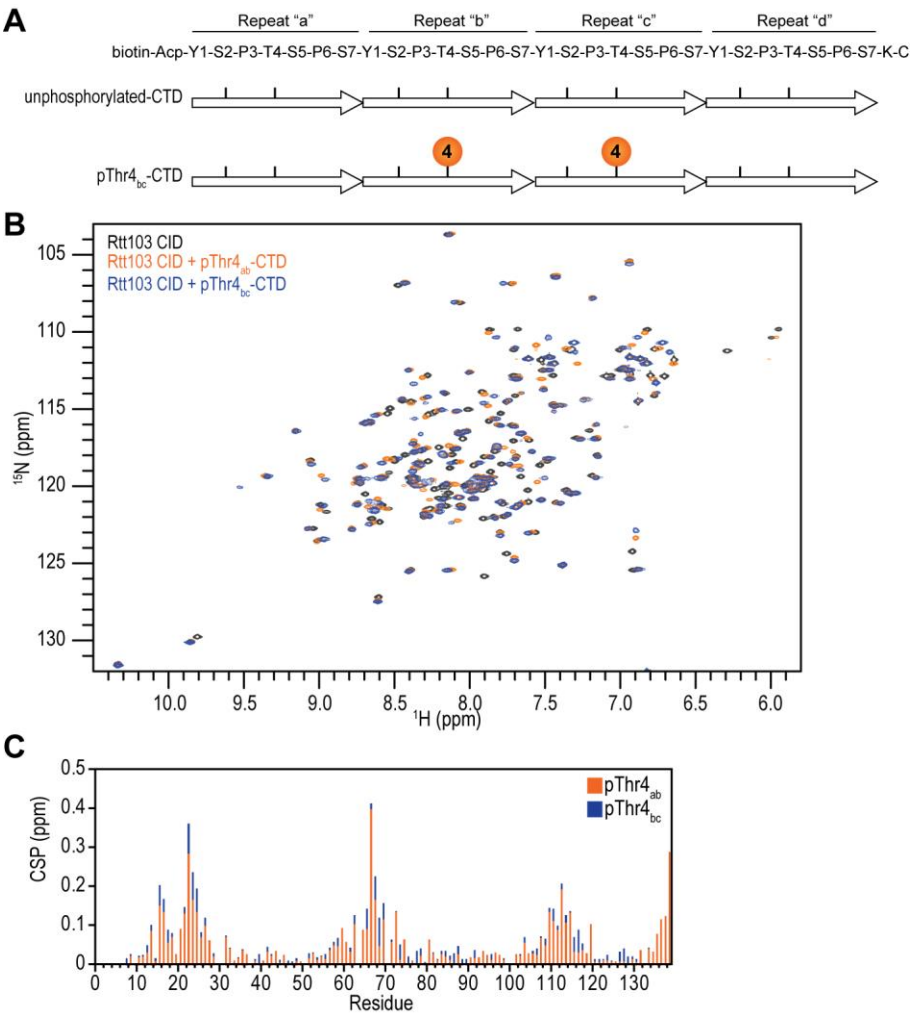

Fig. S7 Additional NMR data. (*A*) A schematic of additional CTD peptides used in NMR titrations is shown. Phosphothreonines are indicated by orange circles. (*B*) Overlay of ^{1}H-^{15}N HSQC spectra of free Rtt103-CID (black) or in complex with pThr4$_{ab}$-CTD (orange) or pThr4$_{bc}$-CTD (blue). (*C*) Chemical shift perturbations (CSP) of Rtt103-CID with two-repeat pThr4$_{ab}$-CTD (orage) or four-repeat pThr4$_{bc}$-CTD (blue) are shown, similar to Fig. 4*C*.

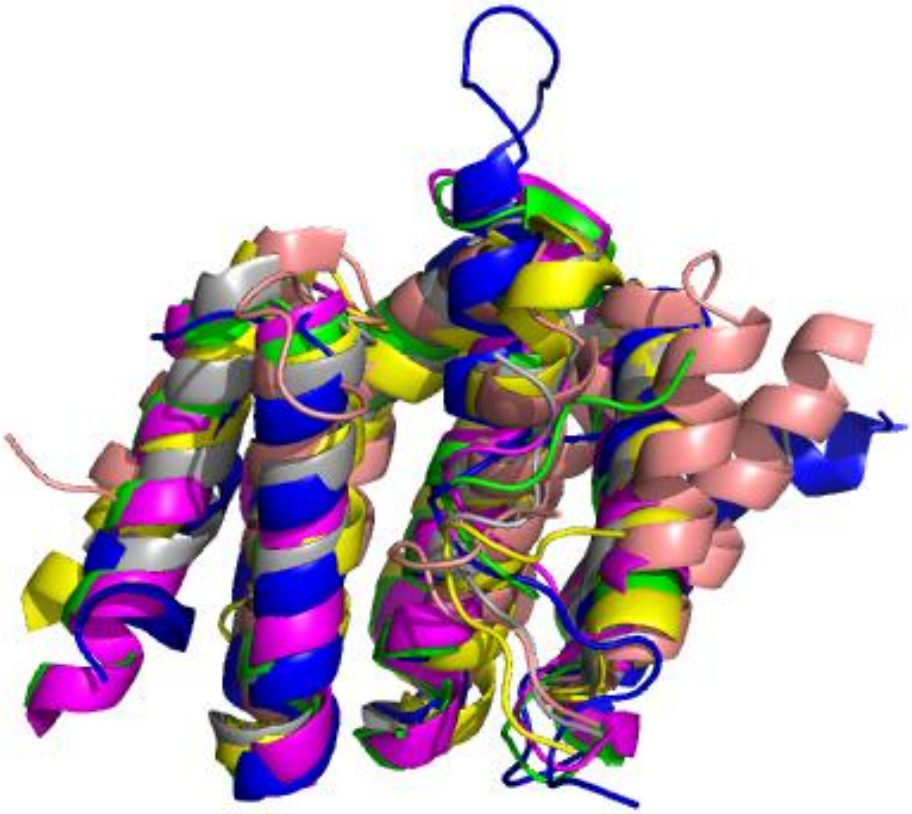

Fig. S8. Superposition of CTD-interacting-domain (CID) structures. Structures were superposed in PyMOL (17). Structures shown are Rtt103 bound to pSer2 (yellow) (PDB 2L0I) (15), Nrd1 bound to pSer5 (blue) (PDB 2LO6) (18), SCAF8 bound to pSer2 and pSer5 (green) (PDB 3D9K) (19), SCAF8 bound to pSer2 and pSer7 (magenta) (PDB 3D9N) (19), Pcf11 bound to pSer2 (salmon) (PDB 1SZA) (20), and RPRD1A bound to pSer7 (grey) (PDB 4JXT) (21).

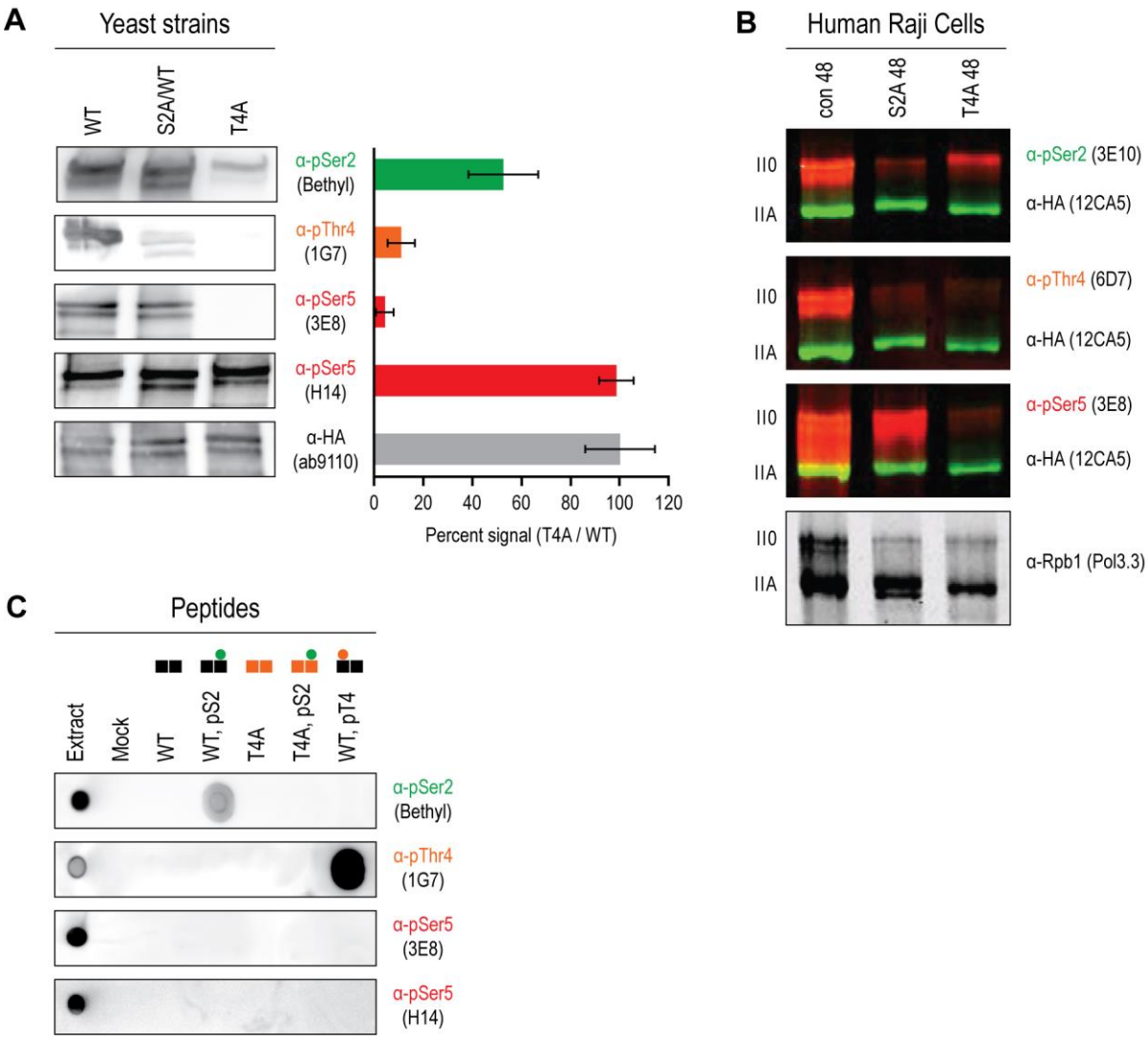

Fig. S9 CTD antibody specificity. (*A*) The phosphorylation state of *S. cerevisiae* cells expressing Pol II bearing either WT, S2A/WT, or T4A CTDs were examined using the indicated CTD-specific antibodies. Quantification of the signal in T4A, normalized to the signal in WT, is shown to the right. Error bars represent SD of three independent replicates. With the H14 antibody, we observe no reduction in pSer5 marks in the T4A strain, suggesting that the observed snoRNA defects are not due to loss of pSer5. We also confirm previous reports that 3E8 antibody requires an intact Thr4 sidechain to bind pSer5 (22). We do observe ~45% reduction in pSer2 levels (Bethyl). (*B*) Similar assay as (*A*), using Human Raji cells. Western blot analysis of Raji whole cell extracts 48h after induction and 24h after α-amanitin using mAbs specific for pSer2 (3E10), pThr4 (6D7), pSer5 (3E8), or Rpb1 (Pol3.3), red signals. Induction was analyzed using the HA mAb (12CA5) (green). The hyper- (II0) and hypo-phosphorylated forms (IIA) of Pol II are indicated. A similar drop (~50%) in pSer2 was observed in T4A 48. Similarly, a near complete loss of pSer5 was observed using the 3E8 antibody. (*C*) Dot blots of chemically synthesized peptides of WT (black) or T4A (orange) CTD repeats, bearing no phosphate, pSer2 (green dots), or pThr4 (orange dots), probed with the indicated CTD antibodies. We observe that the T4A peptide bearing pSer2 was poorly recognized by the Bethyl pSer2 antibody. Thus, we cannot rule out the possibility that the 45% decrease in pSer2 signal observed with the endogenous CTD from T4A strain may be an artifact of antibody specificity.

Datasets

Dataset 1 Comparison of T4A to short CTD. The differential expression of each gene (T4A vs. WT) was compared to previously published differential expression of a strain with a short CTD (CTD11 vs. WT) (16). Genes in both datasets were compared and plotted.

Dataset 2 Raw label-free quantitative proteomics data.

References

1. Kim M, *et al.* (2006) Distinct pathways for snoRNA and mRNA termination. *Mol. Cell* 24(5):723-734.
2. Tietjen JR, *et al.* (2010) Chemical-genomic dissection of the CTD code. *Nat. Struct. Mol. Biol.* 17(9):1154-1161.
3. Steinmetz EJ, *et al.* (2006) Genome-wide distribution of yeast RNA polymerase II and its control by Sen1 helicase. *Mol. Cell* 24(5):735-746.
4. Mayer A, *et al.* (2010) Uniform transitions of the general RNA polymerase II transcription complex. *Nat. Struct. Mol. Biol.* 17(10):1272-1278.
5. Mayer A, *et al.* (2012) CTD tyrosine phosphorylation impairs termination factor recruitment to RNA polymerase II. *Science* 336(6089):1723-1725.
6. Gu MX, Naiyachit Y, Wood TJ, & Millar CB (2015) H2A.Z marks antisense promoters and has positive effects on antisense transcript levels in budding yeast. *BMC Genomics* 16(1):99.
7. Churchman LS & Weissman JS (2011) Nascent transcript sequencing visualizes transcription at nucleotide resolution. *Nature* 469(7330):368-373.
8. Zhang Y, Wen Z, Washburn MP, & Florens L (2010) Refinements to label free proteome quantitation: how to deal with peptides shared by multiple proteins. *Anal Chem* 82(6):2272-2281.
9. Choi H, Fermin D, & Nesvizhskii AI (2008) Significance analysis of spectral count data in label-free shotgun proteomics. *Mol. Cell. Proteomics* 7(12):2373-2385.
10. Ghaemmaghami S, *et al.* (2003) Global analysis of protein expression in yeast. *Nature* 425(6959):737-741.
11. Tomson BN, *et al.* (2013) Effects of the Paf1 complex and histone modifications on snoRNA 3'-end formation reveal broad and locus-specific regulation. *Mol. Cell. Biol.* 33(1):170-182.
12. Grzechnik P, Gdula MR, & Proudfoot NJ (2015) Pcf11 orchestrates transcription termination pathways in yeast. *Genes Dev.* 29(8):849-861.
13. Nonet M, Sweetser D, & Young RA (1987) Functional redundancy and structural polymorphism in the large subunit of RNA polymerase II. *Cell* 50(6):909-915.
14. West ML & Corden JL (1995) Construction and analysis of yeast RNA polymerase II CTD deletion and substitution mutations. *Genetics* 140(4):1223-1233.
15. Lunde BM, *et al.* (2010) Cooperative interaction of transcription termination factors with the RNA polymerase II C-terminal domain. *Nat. Struct. Mol. Biol.* 17(10):1195-1201.
16. Aristizabal MJ, *et al.* (2013) High-throughput genetic and gene expression analysis of the RNAPII-CTD reveals unexpected connections to SRB10/CDK8. *PLoS Genet.* 9(8):e1003758.
17. Schrödinger L (2010) The PyMOL Molecular Graphics System, Version 1.3.
18. Kubicek K, *et al.* (2012) Serine phosphorylation and proline isomerization in RNAP II CTD control recruitment of Nrd1. *Genes Dev.* 26(17):1891-1896.
19. Becker R, Loll B, & Meinhart A (2008) Snapshots of the RNA processing factor SCAF8 bound to different phosphorylated forms of the carboxyl-terminal domain of RNA polymerase II. *J. Biol. Chem.* 283(33):22659-22669.
20. Meinhart A & Cramer P (2004) Recognition of RNA polymerase II carboxy-terminal domain by 3'-RNA-processing factors. *Nature* 430(6996):223-226.
21. Ni Z, *et al.* (2014) RPRD1A and RPRD1B are human RNA polymerase II C-terminal domain scaffolds for Ser5 dephosphorylation. *Nat. Struct. Mol. Biol.* 21(8):686-695.
22. Schwer B, Sanchez AM, & Shuman S (2012) Punctuation and syntax of the RNA polymerase II CTD code in fission yeast. *Proc Natl Acad Sci U S A* 109(44):18024-18029.